AU J.T. 10(1): 55-62 (Jul. 2006)

Transient Free Convection Generated by a Heated Vertical Plate in a Rectangular Cavity

S.A. Ayo

Department of Mechanical Engineering, Federal University of Technology Minna, Nigeria

Abstract

The effects of aspect ratio on the transient free convection generated by a heated vertical plate in a rectangular cavity is investigated for the characteristics and rates of heat transfer from the plate into the surrounding fluid medium. The plate is assumed to be an isothermal plate at a high temperature, suddenly immersed in air at a lower temperature inside the cavity whose walls are also assumed to be adiabatic. The full two-dimensional time-dependent partial differential forms of the conservation equations of continuity, momentum, and energy governing the flow field are cast and solved by a numerical method employing the finite-difference scheme. During the initial short period, heat flow is found to be by conduction irrespective of aspect ratio. The conduction regime is found to be more prolonged for tall enclosures. Shortly after conduction sets in the convection indicated by increase in the heat transfer coefficient following a temporal minimum in the coefficient at the end of the conduction regime. The rate of heat transfer by convection is found to increase with aspect ratio. At large times the temperature field stratifies and the heat transfer to the medium approaches zero, the velocity field decaying gradually and the flow approaches its eventual quiescence.

Keywords: *Transient, free convection, rectangular cavity, heated vertical plate, aspect ratio, isothermal, adiabatic*

Introduction

Various researches have been conducted on the phenomenon of transient free convection generated by heated vertical plates in fluid media. These researches have employed experimental as well as analytical methods, the analytical methods assuming various configurations and adopting different approaches of solution such as closed form and numerical methods.

Khalilolahi & Sammakia (1986) used the simple arbitrary Langrangian-Eulerian (SALE) technique to analyze the full two-dimensional equations representing mass, momentum, and energy balance for unsteady buoyancy-induced flow generated by an isothermal vertical surface enclosed in a long rectangular cavity. He considered the plate to be centrally located and used symmetry to analyze the flow for one-half of the enclosure. He observed the quasi-one-dimensional conduction regime adjacent to the surface at very short times, the steady boundary-layer flow near a semi-infinite surface in an infinite media at intermediate times, and at later times, stratification of temperature field as flow approaches its eventual quiescence. Eseki et al (1993) studied the cases of flow generated by an isothermal vertical surface and one with constant heat flux in a square cavity with the base adiabatic and other walls at a constant cold temperature. He discovered that for the case of the isothermal surface, the heat flux on the opposite side of the hot surface increases when the surface is moved from a position very close to the left side vertical bounding walls towards the vertical line of symmetry of the plate and the rate decreases as the line of symmetry is approached. The same result was observed at the right side bounding walls. He further reported that for a vertical shift of the plate, for high Ra, ($Ra \geq 3 \times 10^6$) the maximum heat

transfer rate occurs when the plate is located at one-third of the height of the cavity. For Ra about 10^6 only small changes in the heat transfer rate occurs, and for lower Ra. (Ra. $\leq$ 10^6) significant changes in the rate of heat transfer are introduced, with the maximum occurring closer to the top of the cavity.

Sammakia et al (1980) conducted both experimental and analytical (numerical) investigation on transient natural convection generated by a semi-infinite surface in air and in water, and the results from the two showed close agreement especially for the laminar flow regime. Hellums and Churchill (1962) used an explicit finite-difference scheme to solve the full boundary layer equations in their time-dependent partial differential forms representing the flow field adjacent to a semi-infinite flat vertical isothermal surface in an infinite medium. The results were in excellent agreement with the early analysis due to Ostrach (1972). Also, the results for measurements by Gebhart and Adams (1962) agree well with those of the integral method of Gebhart (1961) in the analysis of transients adjacent to a semi-infinite vertical plate.

The present work focuses on transient free convection generated in a rectangular cavity with a source of heat, an isothermal vertical plate located within the cavity. Motivation for this study has been aroused by the observed early heat accumulation tendencies of electronic components in sealed enclosures, which could have adverse effect on the performance of the devices. The research seeks to investigate the various regimes of heat transfer and their characteristics, and the rates of heat transfer, defined in quantitative terms, from the surfaces as a function of aspect ratio.

In the study, the full two-dimensional conservation equations governing the flow field are numerically analyzed assuming adiabatic conditions. Although natural convection in enclosure is necessarily three-dimensional and finite heat transfer occurs across the walls, at sections sufficiently deep in the horizontal direction, the flow is essentially two-dimensional and the assumption of adiabatic boundary conditions is appropriate because usually the boundaries are much worse conductors of heat than the fluid.

Mathematical Formulation

The physical problem is modelled as a two-dimensional rectangular cavity with adiabatic walls on all sides, filled with air (see figure 1) below. The hot plate is an isothermal element of negligible thickness oriented vertically inside the cavity. At the initial time, the fluid, the plate, and the bounding walls are all at the same initial ambient temperature, T_i, until suddenly the temperature of the plate is raised and maintained at a higher, uniform and constant value, T_w.

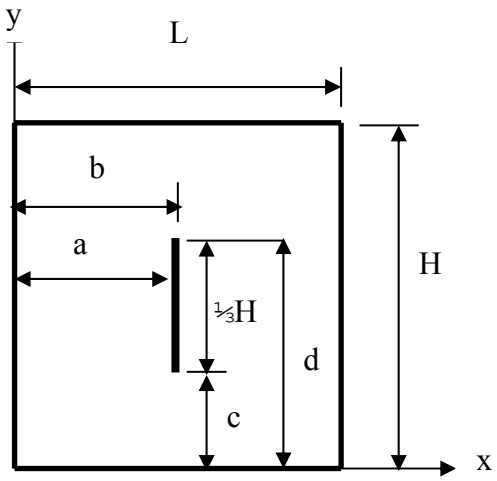

Fig. 1. The physical model

The following assumptions are made in order to simplify the analysis of the problem:

(i) The flow is laminar and two-dimensional
(ii) The fluid is Newtonian, viscous, and incompressible
(iii) Fluid properties are constant except in the buoyancy term consideration
(iv) Viscous dissipation term is negligible
(v) Heat flow by radiation is negligible
(vi) No internal heat source or heat sink is involved
(vii) The walls are impermeable and the no-slip condition applies.

The appropriate equations governing the flow field are the conservation equations of mass, momentum, and energy;

$$\frac{\partial u}{\partial x}+\frac{\partial v}{\partial y}=0 \qquad (1)$$

$$\frac{\partial u}{\partial t}+u\frac{\partial u}{\partial x}+v\frac{\partial u}{\partial y}=-\frac{1}{\rho}\frac{\partial p}{\partial x}+\nu\nabla^2 u \qquad (2)$$

$$\frac{\partial v}{\partial t}+u\frac{\partial v}{\partial x}+v\frac{\partial v}{\partial y}=-\frac{1}{\rho}\frac{\partial p}{\partial y}+\nu\nabla^2 v+F_y \quad (3)$$

$$\frac{\partial T}{\partial t}+u\frac{\partial T}{\partial x}+v\frac{\partial T}{\partial y}=\alpha\nabla^2 T \quad (4)$$

where,
u is horizontal component of velocity
v is vertical component of velocity
T is temperature
t is time
y is vertical coordinate
x is horizontal component
ρ is density of fluid inside the heated layer
p is pressure
ν is the kinematic viscosity of the fluid
α is the thermal diffusivity

The body force due to buoyancy in the y-direction can be obtained by the Boussisesqu approximation,

$$\rho=\rho_o(1+\beta\Delta T) \quad (5)$$

where,
β is the volume coefficient of thermal expansion
ρ_o is the bulk fluid density,
ΔT is the temperature difference between the heated layer and the bulk value,
The body force per unit mass, F_y, due to buoyancy in the y-direction is thus,

$$F_y=-\beta g(\Delta T)$$

where, g is the acceleration due to gravity.
The y-momentum equation becomes,

$$\frac{\partial v}{\partial t}+u\frac{\partial v}{\partial x}+v\frac{\partial v}{\partial y}=-\frac{1}{\rho}\frac{\partial p}{\partial y}+\nu\nabla^2 v-\beta g(\Delta T) \quad (6)$$

Boundary and Initial Conditions

The above governing equations are subject to the following initial and boundary conditions:
at t = 0, u = v = T – T_i = 0,
for t > 0,

u = v = T – T_w = 0 at $\begin{cases} x = a \\ x = b, \end{cases}$ and c <y < d,

u = v = $\partial T/\partial x$ = 0 at $\begin{cases} x = 0 \\ x = L, \text{ and } 0 \le y \le H \end{cases}$

u = v = $\partial T/\partial y$ = 0 at 0 < x < L and $\begin{cases} y = 0 \\ y = H \end{cases}$

Normalization of the Governing Equations

Following Khalilolahi and Sammakia (1986), the equations are made dimensionless using the following non-dimensionalizing parameters:
X = x/L; Y = y/L; U = uL/ν; V = vL/ν; τ = tν/L^2; $\theta = (T-T_i)/(T_w-T_i)$; $P = PL^2/\rho\nu^2$
where,
Y is dimensionless vertical coordinate
X is dimensionless horizontal coordinate
U is dimensionless horizontal component of velocity
V is dimensionless vertical component of velocity
T_i is initial temperature of fluid, plate & wall
T_w is temperature of isothermal surface
θ is dimensionless temperature
τ is dimensionless time
P is dimensionless pressure

The dimensionless form of the equations and the boundary and initial conditions are thus as follows:

$$\frac{\partial U}{\partial X}+\frac{\partial V}{\partial Y}=0 \quad (7)$$

$$\frac{\partial U}{\partial \tau}+U\frac{\partial U}{\partial X}+V\frac{\partial U}{\partial Y}=-\frac{\partial P}{\partial X}+\frac{\partial^2 U}{\partial X^2}+\frac{\partial^2 U}{\partial Y^2} \quad (8)$$

$$\frac{\partial V}{\partial \tau}+U\frac{\partial V}{\partial X}+V\frac{\partial V}{\partial Y}=-\frac{\partial P}{\partial Y}+\frac{\partial^2 V}{\partial X^2}+\frac{\partial^2 V}{\partial Y^2}+Gr\theta \quad (9)$$

$$\frac{\partial \theta}{\partial \tau}+U\frac{\partial \theta}{\partial X}+V\frac{\partial \theta}{\partial Y}=\frac{1}{\mathrm{Pr}}\left(\frac{\partial^2 \theta}{\partial X^2}+\frac{\partial^2 \theta}{\partial Y^2}\right) \quad (10)$$

where, $Gr = g\beta(T_w - T_i)L^3/\nu^2$
$\mathrm{Pr} = c_p\mu/k$
β is volume coefficient of thermal expansion
c_p is specific heat at constant pressure
μ is dynamic viscosity of fluid
k is thermal conductivity

Dimensionless Boundary and Initial Conditions

The normalized boundary and initial conditions are:
at τ = 0, U = V = θ = 0,
for τ > 0,

U = V = θ – 1 = 0 at $\begin{cases} X = a/L \\ X = b/L, \text{ \& } c/L < Y < d/L \end{cases}$

$$U = V = \partial\theta/\partial Y = 0 \text{ at } \begin{cases} X = 0 \\ X = 1 \text{ and } 0 \le Y \le H/L \end{cases}$$

$$U = V = \partial\theta/\partial Y = 0 \text{ at } 0 < X < 1, \text{ and } \begin{cases} Y = 0 \\ Y = H/L \end{cases}$$

The Vorticity Transport Equation

The normalized X- and Y- momentum equations are combined together to eliminate the pressure terms, to yield the normalized vorticity transport equation as,

$$\frac{\partial\omega}{\partial\tau} + U\frac{\partial\omega}{\partial X} + V\frac{\partial\omega}{\partial Y} = \frac{\partial^2\omega}{\partial X^2} + \frac{\partial^2\omega}{\partial Y^2} + Gr\frac{\partial\theta}{\partial X} \quad (11)$$

where, ω is dimensionless vorticity

The Poisson Equation for Stream Function

The vorticity transport equation above does not have any explicit boundary conditions for evaluating the vorticities. To solve the problem therefore, the Poisson equation for the stream function, and the velocity-stream function equations are introduced as a means of determining the vorticities at the boundaries. The approach also enables the values of the streamlines within the domain to be generated. The normalized form of the equations conforming with the normalized parameters above are expressed as follows:

$$\frac{\partial^2\psi}{\partial X^2} + \frac{\partial^2\psi}{\partial Y^2} = -\omega \quad (12)$$

$$\frac{\partial\psi}{\partial Y} = U \quad (13a); \quad \frac{\partial\psi}{\partial X} = -V \quad (13b)$$

subject to the following dimensionless initial and boundary conditions:

at $\tau = 0$, $\omega = \psi = 0$,

for $\tau > 0$,

$$\psi = 0 \text{ at } \begin{cases} X = a/L \\ X = b/L, \text{ and } c/L < Y < d/L, \end{cases}$$

$$\text{at } \begin{cases} X = 0 \\ X = 1 \text{ and } 0 \le Y \le H/L \end{cases}$$

$$\text{at } 0 < X < 1, \text{ and } \begin{cases} Y = 0 \\ Y = H/L \end{cases}$$

where, ψ is dimensionless streamfunction

Vorticity Boundary Conditions

Following Shoichiro (1977) the vorticities at the walls are obtained by expanding the streamfunction values at points adjacent to the walls in the Taylor's series about the walls. After necessary simplifications, the boundary vorticities are approximated by,

$$\omega_{wall} = -\frac{2}{\Delta n^2}(\psi_{wall+\Delta n})$$

Δn is a subdivision (ΔX or ΔY) on the axis normal to the surface, taken from the surface into the fluid medium.

At the sharp concave corners, 'b', 'd', 'f', and 'h',

$$\frac{\partial V}{\partial X} = 0; \quad \frac{\partial U}{\partial Y} = 0$$

so that at the corners the vorticities vanish, i.e.,

$$\omega_b = \omega_d = \omega_f = \omega_h = 0$$

Numerical Method of Solution

The numerical method adopted for solving the system of partial differential equations is the finite difference. The entire domain is subdivided into a mesh system, size m x n, with uniform divisions, ΔX and ΔY, in the X- and Y-directions respectively, ensuring that the boundaries lie on grid points. Because of the derivative boundary conditions, four fictitious lines, two horizontal, distance ΔY top and bottom of the cavity, and two vertical, distance ΔX left and right of the cavity are introduced.

The appropriate finite-difference scheme representations of the partial differential terms in the governing equations are cast and used to replace each of the terms, the central difference approximation being used in the space derivatives, and the forward difference in the time derivatives. Equations 10, 11 and 13 are expressed explicitly, and equation 12 implicitly. The system of discretized equations are then solved numerically starting from time $\tau = 0$, and marched in time, using a sufficiently small time step that allows for the stability of the solution, until a desired time is reached. The Von Neumann stability analysis is used in determining the stability criteria.

The system of equations 10, 11, 12, and 13 are solved following a cyclical sequence. During any one time step, the energy transport equation, equation 10, is solved first for θ using the initial values of U, V, and θ. In the next

stage and for the same time step, the vorticity transport equation , equation 11, is solved for ω at the interior of the domain, still using the same initial values of U and V but the new values of θ obtained from the solution of equation 10, leaving the vorticities at the boundaries. These most recent values of ω are used in the Poisson equation for stream function, equation 12, to yield a system of simultaneous equations which is now solved for by an iterative scheme to obtain the values of ψ still for the same time step. The vorticities at the boundaries are then evaluated using the values of ψ at the adjacent nodal points perpendicular to the surface. And lastly the X- and Y-velocity equations, equations 13a & 13b, are solved using the values ψ obtained at the last stages. This completes the first cycle of operations for the first time step. For the second cycle, the values obtained in the first cycle are used to repeat the entire operations again to obtain new distributions for θ, ω, ψ, etc. This operation is repeated until the desired time is reached.

The iterative scheme adopted for solving the implicit stream function equation is the Liebmann iterative method accelerated by the Successive Over-relaxation, (S.O.R), method for convergence. Following Chuen-Yen (1979) the convergence of the stream function equation is subject to the criterion,

$$\sum_{i=2}^{m}\sum_{j=2}^{n}\left|\psi_{i,j}^{t+1}-\psi_{i,j}^{t}\right| \le \delta$$

where, δ is the residue taken as $1x10^{-04}$

Heat Transfer Calculation

The effect of fluid motion on the rate of heat transfer from the hot surface into the fluid medium is expressed in terms of Nusselt numbers. The Nusselt number is evaluated at specific points as local Nusselt number, or averaged over one of the plate surfaces as local mean Nusselt number, or over the entire surface as overall mean Nusselt number.

The local mean Nusselt numbers at the sides, and bottom and top of the plate are therefore expressed respectively as,

$$Nu = -\frac{\partial\theta}{\partial X}; \quad Nu = -\frac{\partial\theta}{\partial Y}$$

And the overall mean Nusselt number is expressed as

$$\overline{Nu} = \frac{\left(\overline{Nu_R}+\overline{Nu_L}\right)\left(d_j-c_j+1\right)+\left(\overline{Nu_B}+\overline{Nu_T}\right)\left(b_i-a_i+1\right)}{2\left(d_j-c_j+1\right)\left(b_i-a_i+1\right)}$$

Where, a_i and b_i, and c_j and d_j are respectively the X- and Y-coordinates of the corners of the plate. Nu_L and Nu_R are respectively the mean Nusselt numbers at the left and right sides of the plate, while Nu_T and Nu_B are respectively the mean Nusselt numbers at the top and bottom of the plate expressed as

$$\overline{Nu_L} = -\frac{1}{L_p}\int_{c_j}^{d_j}\frac{\partial\theta}{\partial X}dY\Big|_{x=n}$$

$$\overline{Nu_R} = -\frac{1}{L_p}\int_{c_j}^{d_j}\frac{\partial\theta}{\partial X}dY\Big|_{x=b}$$

$$\overline{Nu_T} = -\frac{1}{B_p}\int_{a_j}^{h_j}\frac{\partial\theta}{\partial Y}dX\Big|_{Y=d}$$

$$\overline{Nu_B} = -\frac{1}{B_p}\int_{a_j}^{h_j}\frac{\partial\theta}{\partial Y}dX\Big|_{Y=c}$$

$L_p = d - c$; $B_p = b - a$

The mean Nusselt numbers are evaluated using the trapezoidal rule.

Results and Discussion

The results of the numerical study of transient free convection generated by a heated vertical plate in a rectangular air cavity are presented. Results are presented for the effects of aspect ratio on heat transfer from the plate surface. The investigation was conducted for Pr. No. = 0.72, and heated plate of length, L_p = (1/3) H but negligible width. A maximum Grashof number, Gr. = 4.65E+06, which allows for the stability of the numerical scheme has been employed. This implies a Raleigh number, Ra = 3.35E+06, corresponding to a laminar flow regime.

Figs. 2-4, respectively, present the effects of aspect ratio on heat transfer by comparing the variation of mean Nusselt number with time for various aspect ratios for two values of Grashof number (Gr = 46500 and Gr = 465000), and plate centrally located. It would be observed from the figures that the

curves are collinear and have same steepness at very small times, $\tau < 0.0004$, irrespective of the aspect ratio. This indicates that aspect ratio does not have effect on the rate and mode of heat transfer, which is quasi-one-dimensional at very small initial periods. This is in agreement with the earlier study due to Khalilolahi and Sammakia (1986). Shortly after the initial times, the curves begin to deviate from the one-dimensional trend to undergo temporal minima which indicates the onset of convection, with those for the lower aspect ratios leading the deviation and the process of temporal minimum. This indicates therefore that convection sets in earlier for shallow cavities than tall ones. In other words longer conduction regimes and therefore a tendency for higher heat accumulation is associated with tall enclosures at very small times. This may be due to the fact that for tall enclosures there exist greater freedom at the top of the cavity for redistribution of energy conducted to the top that only a thin layer of the fluid parallel and close to the plate surface is involved in the heat transfer process. The fluid elements continue to move parallel to the plate surface so that heat transfer is at molecular level as in any conduction heat transfer process. For shallow cavities the space at the top of the cavity is restricted and therefore a progressively larger column of fluid is drafted to take part in the heat transfer process at a much earlier period, giving rise to early convection.

As convection proceeds the curves tend to behave in reverse manner – the higher aspect ratio curves now exhibiting higher rates of heat transfer than the lower ones. This indicates that though convection may be delayed for tall cavities, but once it is commenced it progresses with greater vigour than there occurs for shallow cavities. Figures 5a – c and figures 6a – c compare the isothermals for H/L = 1/2 & H/L= 1 at corresponding times. It would be observed from figures 5a & 6a that at corresponding time τ= 36E -04 the isotherms for H/L = 1 (fig. 6a) show uniform heat transfer in all directions typical of the one-dimensional conduction regime while those for H/L = ½ (fig. 5a) indicate deviation from the one-dimensional trend (onset of convection). The isotherms of figure 6c are already beginning to

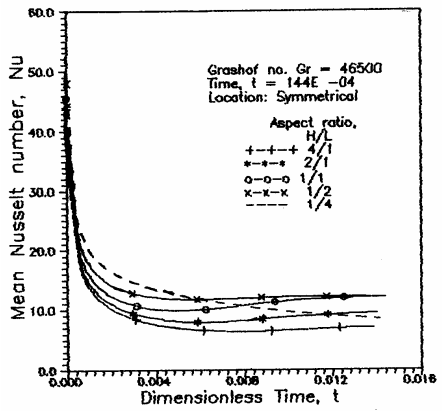

Fig. 2. Variation of mean Nusselt number with time for various aspect ratios

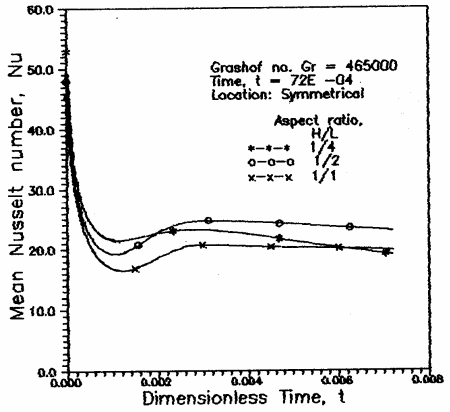

Fig. 3. Variation of mean Nusselt number with time for various aspect ratios

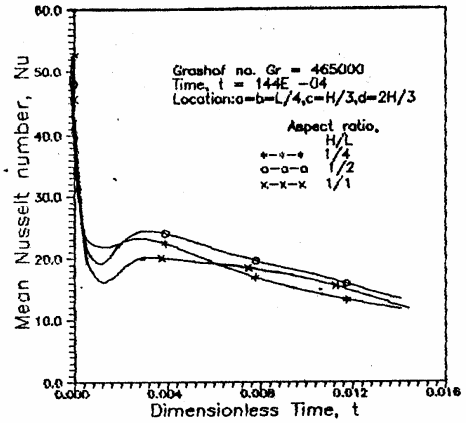

Fig. 4. Variation of mean Nusselt number with time for various aspect ratios

show thermal stratification at time τ = 288E -04 well ahead of those for H/L = ½ (fig. 5c) at the same time. It would also be seen from the figures that thermal energy reaches to the bounding vertical walls earlier for H/L = 1 than for H/L = 1/2 at corresponding times. This shows that convection reaches to the vertical bounding walls earlier for tall cavities notwithstanding the initial slow rate of

propagation. This could be due to the shorter dimension in the horizontal direction that convection would have to traverse before reaching the vertical bounding walls of tall enclosures. As a result the entire fluid column above the base of the hot plate gets involved in the convection process earlier. As energy continues to be convected into the fluid medium, convection vigour is increased much more above that for shallow cavities to cause higher rates of heat transfer for tall cavities as compared to shallow ones. At such times convection is still progressing in the horizontal direction for shallow enclosures and therefore moderate in intensity.

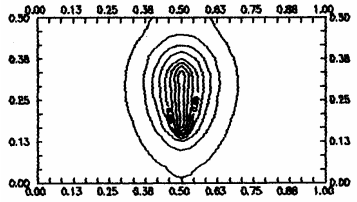

Fig.5a. Time,τ=36E-4

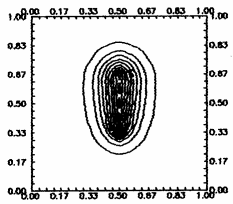

Fig.6a.Time,τ=36E-4

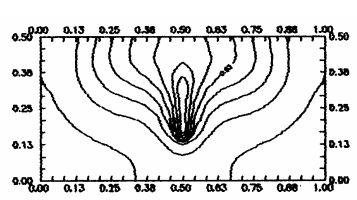

Fig.5b. Time,τ=144E-4

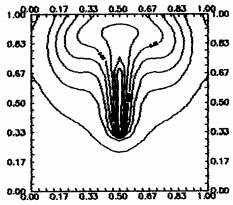

Fig.6b.Time,τ=144E-4

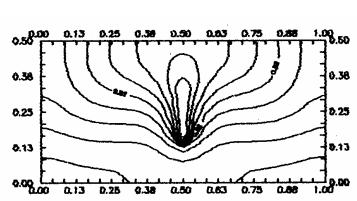

Fig.5c. Time,τ=288E-4

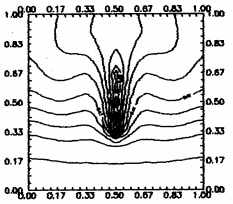

Fig.6c.Time,τ=288E-4

Fig. 5. Isotherms for H/L=1/2.

Fig.6. Isotherms for H/L=1.

Conclusion

In this study it has been demonstrated that in a transient free convection generated by a heated vertical plate in a rectangular air cavity essentially three different regimes of flow are distinguishable: the one-dimensional conduction regime at short times, the convection regime at later times, and thereafter thermal stratification when the flow approaches its eventual quiescence. The conduction heat transfer associated with low rates of heat transfer and therefore a sudden rise in temperature in the vicinity of the plate should therefore be responsible for early heat accumulation tendencies associated with electronic and other similar devices. The conduction regime has been observed to be more prolonged for tall enclosures than shallow ones. It could, thus, be deduced that shallow enclosures support higher rates of heat transfer at small initial times. The converse is the case after onset of convection as tall enclosures now tend to exhibit higher rates of heat transfer over shallow ones which is due to the high convection vigour associated with tall cavities after the onset of convection.

References

Chuen–Yen C., (1979), An Introduction to Computational Fluid Mechanics, John Wiley & Sons, New York.

Eseki, M. H., Reises, J. A., and Behnia, M., (1993), Natural Convection Heat Transfer from Electronic Components Located in an Enclosure, The 6th. International Symposium on Transport Phenomena in Thermal Engineering, Seoul, Korea, pp. 249 – 254.

Gebhart, B., (1961), Transient Natural Convection from Vertical Elements, ASME JOURNAL OF HEAT TRANSFER, pp. 61 – 70.

Gebhart, B., and Adams, D. E., (1962), Measurements of Transient Natural Convection in Flat Vertical Surfaces, ASME JOURNAL OF HEAT TRANSFER, Vol. 83, pp. 1 – 4.

Hellums, J. D., and Churchill, S. W., (1962), Transient and Steady State, Free and Natural Convection, Numerical Simulations: Part 1. The Isothermal Vertical Plate, AIChE Journal.

Khalilolahi A. and Sammakia B. (1986), Unsteady natural Convection Generated by

a Heated Surface Within an Enclosure, Numerical Heat Transfer, Vol. 9, pp. 715 – 730.

Ostrach S., (1972) , Natural \convection in Enclosures, Advances in Heat Transfer, Vol. 8, pp. 161 – 227.

Sammakia, B., Gebhart, B., and Qureshi, Z. H., (1980), Measurements and Calculations of Transient Natural Convection in Air, Int. J. Heat and Mass Transfer, Vol. 23, pp. 571 – 576.

Shoichiro, N., (1977), Computational Methods in Engineering and Science, John Wiley & Sons Inc., New York.